Free-Radical Initiator-Based Carrier-Free Smart Nanobomb for Targeted Synergistic Therapy of Hypoxic Breast Cancer

Liefeng Hu,[*a, b], Ganlin Dong,[b] Xiaohong Li,[b] Shuting Li,[*c] and Yonggang Lv[*b]

Methods

Materials. 2,2'-azobis[2-(2-imidazolin-2-yl)propane]-dihydrochloride (AIPH), Zinc nitrate hexahydrate (Zn(NO$_3$)$_2$·6H$_2$O), 5,5-dimethyl-1-pyrroline N-oxide (DMPO), and 2,2'-azino-bis(3-ethylbenzothiazoline-6-sulfonic acid) (ABTS) were obtained from Energy Chemicals (Shanghai, China) and used without further purification. ICG was provided by Tokyo Chemical Industry Co., Ltd. (Japan). PEG-FA was purchased from Ponsure Biotechnology (Shanghai, China). *N*, *N*-Dimethylformamide (DMF), and triethylamine (TEA) were purchased from Sinopharm Chemical Reagent (SCR). All reagents were used without further purification. Methyl thiazolyl tetrazolium (MTT), 4',6-diamidino-2-phenyl-indole (DAPI), calcein-AM, propidium iodide (PI) cell apoptosis kit, and lysosomal fluorescent probes were received from Meilun Biotechnology Co., Ltd (Dalian, China). Fetal bovine serum (FBS), Dulbecco's modified Eagle's medium (DMEM) were obtained from Gibco Life Technologies (USA). All cell lines used in this study were obtained from the Chinese Type Culture Collection (Wuhan University). The animals used in the manscript were Female BALB/c mice (16-18g) purchased from the Experimental Animal Center of Huazhong Agricultural University. All animal experiments conformed to the guidelines of the Chinese Regulations for the Administration of Affairs Concerning Experimental Animals and were approved by the Institutional Animal Care and Use Committee of Huazhong Agricultural University, China, and the animal ethics approval number was HZAUMO-2023-0311. Besides, all animal studies in this manuscript conformed to the guidelines of the Animal Research: Reporting In Vivo Experiments (ARRIVE) 2.0 and the general principles set out in the Declaration of Helsinki.

Photothermal effects evaluation of IANM-PEG-FA. 500 μL IANM-PEG-FA aqueous solutions with different concentrations of ICG (0, 1.8, 3.8, 7.5, 15, and 30 μg mL^{-1}) were added into Eppendorf tubes respectively, and then exposed to laser radiation (808 nm, 1 W cm^{-2}) for 3 min. To detect the photothermal performance under different laser power densities, IANM-PEG-FA aqueous solution (500 μL) was irradiated under different powers of 808 nm laser (the power density from 0.15 to 1.00 W cm^{-2}) for 3 min. Subsequently, three cycles of heating and cooling were recorded to test the photothermal stability of the loaded ICG in the IANM-PEG-FA nanosystem, with free indocyanine green (ICG) set as the control group. The real-time records of temperature rise in IANM-PEG-FA solutions were obtained from an infrared thermal imaging camera. In addition, the near-infrared (NIR) fluorescence imaging signature of IANM-PEG-FA was detected by the NIR imager at ICG concentrations of 0-30 μg mL^{-1}.

Cell culture and cellular uptake. The mouse breast cancer cells (4T1) were widely used as hypoxic tumor cells for oxygen-irrelevant therapeutic studies. 4T1 cells were cultured in DMEM medium with the addition of 10% FBS, 1% penicillin/streptomycin in an atmosphere containing 5% CO$_2$ at 37 °C to evaluate the anti-tumor effects of IANM-PEG-FA *in vitro*. To evaluate the FA-mediated active targeting cellular uptake, 4T1 cells were incubated with IANM-PEG-FA (100 μg mL^{-1}) at 37 °C for 1 h, 2 h and 4 h, respectively. And the cell targeting pathway of IANM-PEG-FA was explored using FA pre-treatment to block targeting receptor strategy in 4T1 cells. After washing with PBS, cells were collected and analyzed by confocal laser scanning microscope (CLSM) and flow cytometry. Given the pH responsiveness of IANM-PEG-FA, the lysosomal escape effect was analyzed by localization with a green lysosomal tracker (Lyso-tracker). In addition, 4T1 cells were incubated

with IANM-PEG-FA for 0.5 h-8 h and then centrifuged, washed and lysed, followed by assessment of Zn^{2+} uptake capacity *in vitro* using inductively coupled plasma mass spectrometry (ICP-MS). Meanwhile, the tumor-like three-dimensional (3D) tissues were constructed to assess cargo delivery and penetration effects.

ROS detection in vitro. DCFH-DA was used as the indicator with inverted fluorescence microscope imaging. Briefly, 4T1 cells were seeded in six-well plates under a normoxic and hypoxic environment for 24 h and then incubated with the medium containing PBS, IANM-PEG-FA for another 4 h. For thermally activated free radical-generating cell groups were exposed to a 1 W cm^{-2} 808 nm laser for 3 min. Subsequently, the cells were treated with 10 μM DCFH-DA for 30 min. Notably, ascorbic acid (Vc) acts as a free radical scavenger to inhibit the thermodynamic ability of IANM-PEG-FA, resulting in a single photothermal effect.

Animal studies. To ensure the reliability and reproducibility of the data, all animal studies in the article had a control group and each group of experimental animal units was divided equally into individuals by random sampling method, the sample size of n not less than 3. All animal experimental groups and mice in the article were analyzed in the experimental procedures and results. For easy tumor formation in vivo, the immunodeficient BALB/c mice were selected as animal experimental model, and the mice were housed in specific pathogen free (SPF)-grade animal breeding environment. The experimental mice were carefully cared for by both the experimenter and the breeder.

Infrared thermal imaging. 4T1 tumor-bearing mice were intravenously injected with IANM-PEG-FA or Saline, and then the tumor sites were irradiated with the 808 nm laser at power densities of 1 W cm^{-2} for 5 min with simultaneous imaging by an infrared (IR) thermal camera. For single PTT, Vc was injected intratumorally 4 hours before laser irradiation of the tumor tissue.

Histopathological analysis. Hematoxylin and eosin (H&E) and immunofluorescent staining of terminal deoxynucleotidyl transferase-mediated dUTP-biotin nick end labeling (TUNEL) were performed following the manufacturer's instructions to evaluate histological therapy of the tumors. The prepared slices of tumors were visualized under an inverted fluorescence microscope. For acute toxicity assessment, healthy mice were analyzed for damage to major organs (Heart, Liver, Spleen, Lung and Kidney) by HE staining after injection of high doses (15 mg kg^{-1}) of IANM-PEG-FA through the tail vein.

Statistical Analysis. At least triplicate assays were evaluated. The experimental data are presented as means ± standard deviation (S.D.). The statistical analyses were conducted by a two-tailed Student's t-test. Statistical significance was defined as *, # and & $P < 0.05$, **, ## $P < 0.01$, and ***, ### $P < 0.001$, ns = no significance.
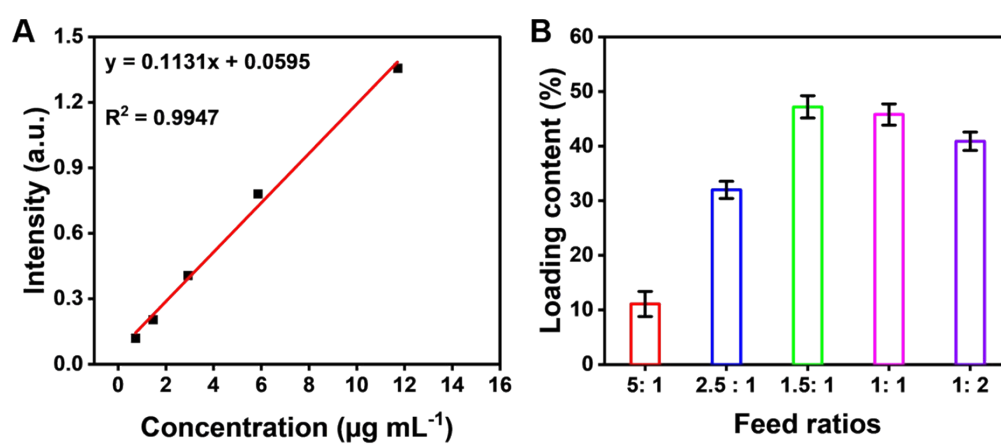
Figures

Fig. S1. The encapsulation properties of ICG. (A) Light absorption calibration of ICG. (B) Variation of ICG loading content with feed ratios.
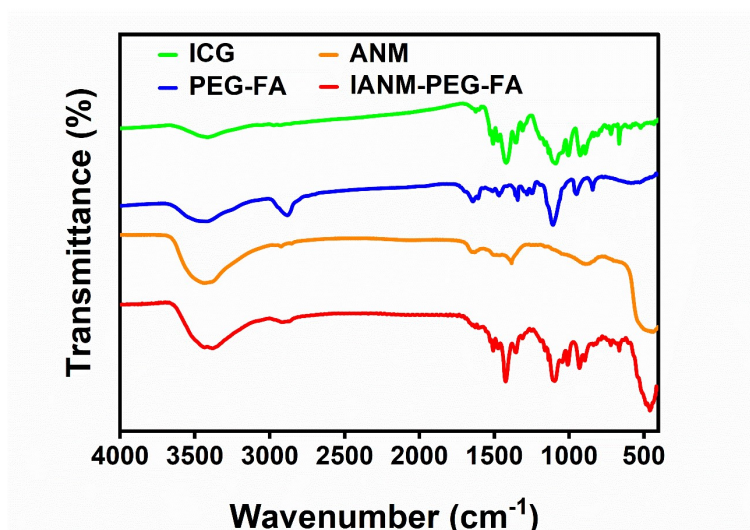

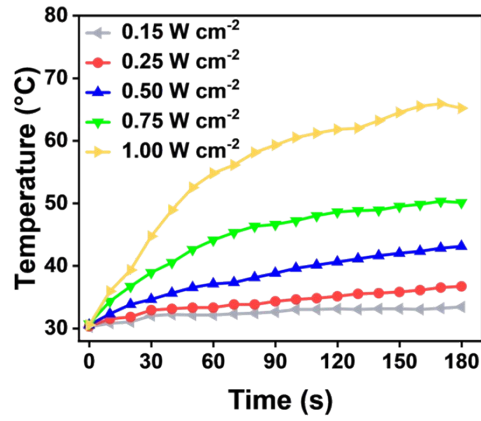**Fig. S2.** FIIR spectra of ICG, ANM, PEG-FA and IANM-PEG-FA.

Fig. S3. Temperature elevation of IANM-PEG-FA in water in dependence of 808 nm laser power density.
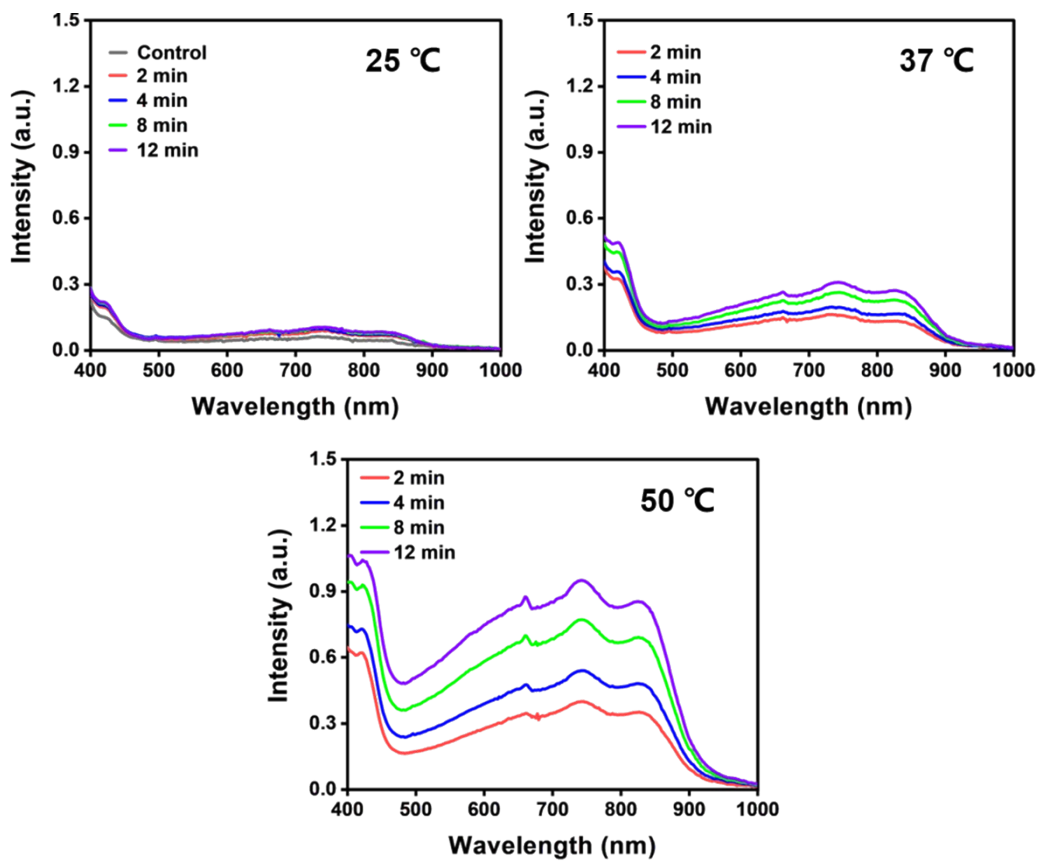

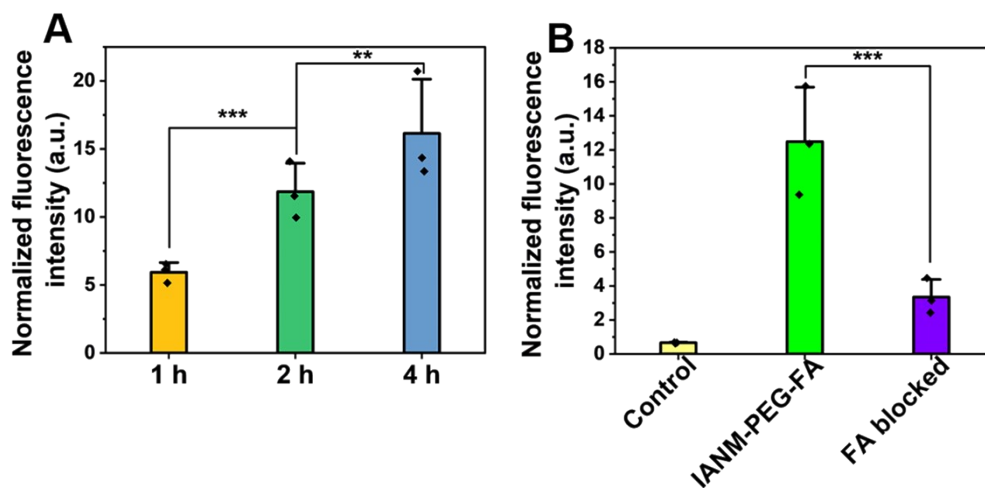**Fig. S4.** The spectra of ABTS$^{+\cdot}$ in the presence of IANM-PEG-FA at different temperature conditions (25, 37 and 50 ℃).

Fig. S5. Semi-quantitative values of fluorescence intensity for cellular uptake. (A) Quantification of cellular uptake after different times (1, 2 and 4 h) of IANM-PEG-FA incubation. (B) Quantification of FA-mediated cell-targeted uptake. Data are presented as mean values ± S.D. (n = 3), and P values are calculated by two-tailed Student's t-test. **$P < 0.01$; ***$P < 0.001$.
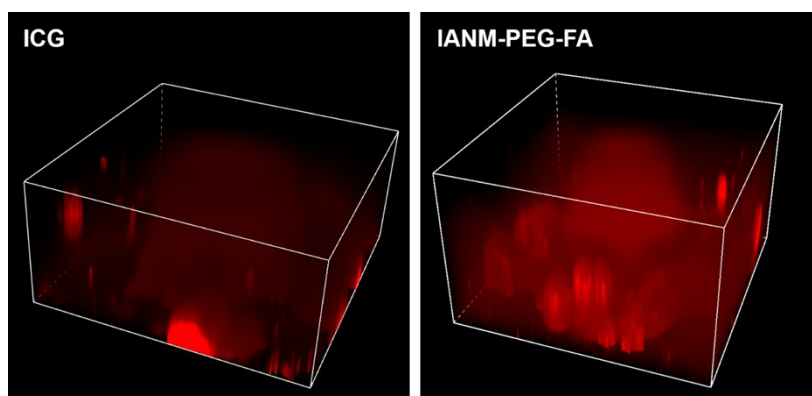
Fig. S6. The full-scan images of ICG and IANM-PEG-FA in MCs.
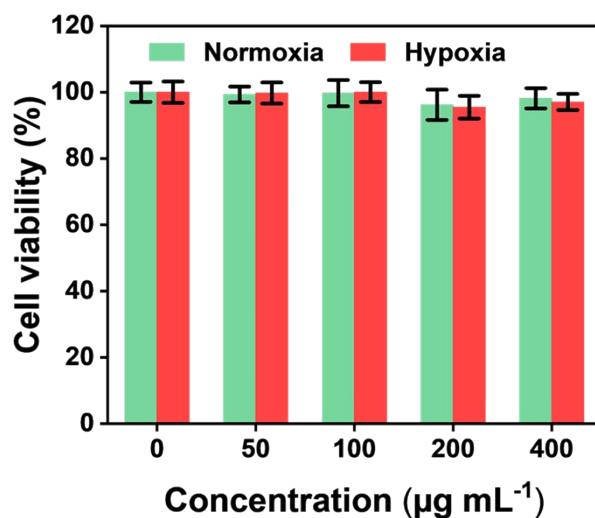
Fig. S7. Cell viability of L929 cells after incubation with different concentrations IANM-PEG-FA under normoxia and hypoxia. Data are given as mean ± S. D. (n = 3).
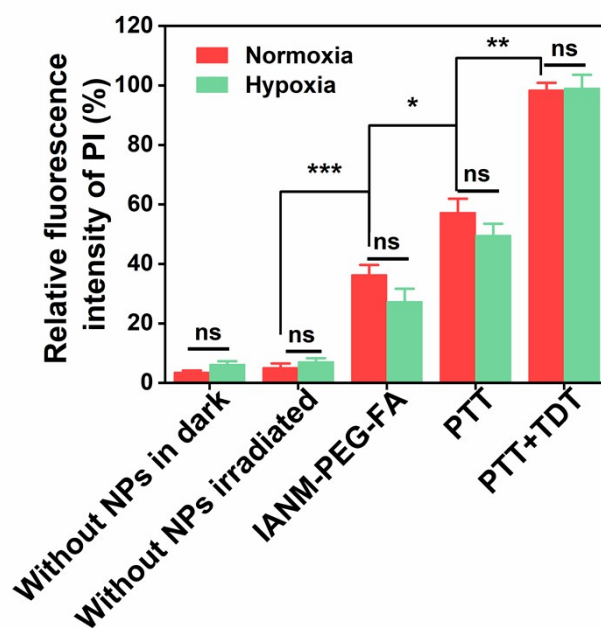
Fig. S8. Quantitative red fluorescence percentage of dead cells. Data are given as mean ± S.D. (n =3), and P values are calculated by two-tailed Student's t-test. ns = no significance; *$P < 0.05$; **$P < 0.01$; ***$P < 0.001$.

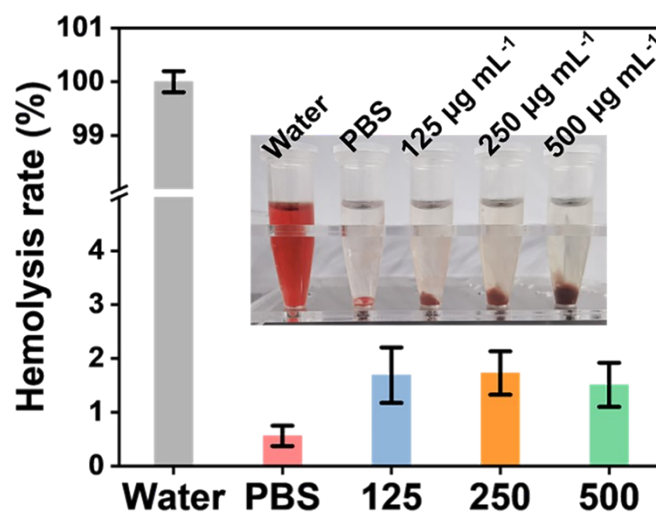**Fig. S9.** The hemolysis rate of IANM-PEG-FA at different concentrations (125, 250, and 500 μg mL^{-1}). The insert images correspond to the optical photos of each group.
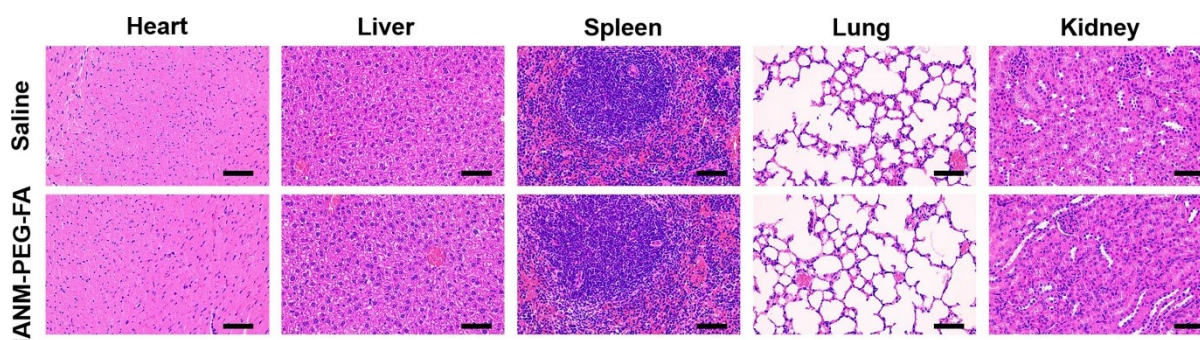
Fig. S10. H&E images of major organ sections from mice after acute toxicity test assessment. Scale bars: 100 µm.
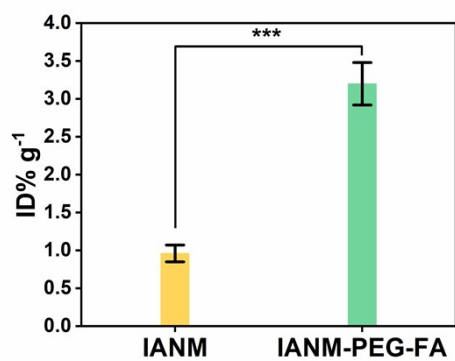

Fig. S11. Quantification of Zn^{2+} content in tumor tissue by ICP-MS. Data are presented as mean values ± S.D., and P values are calculated by two-tailed Student's t-test. ***$P < 0.001$.
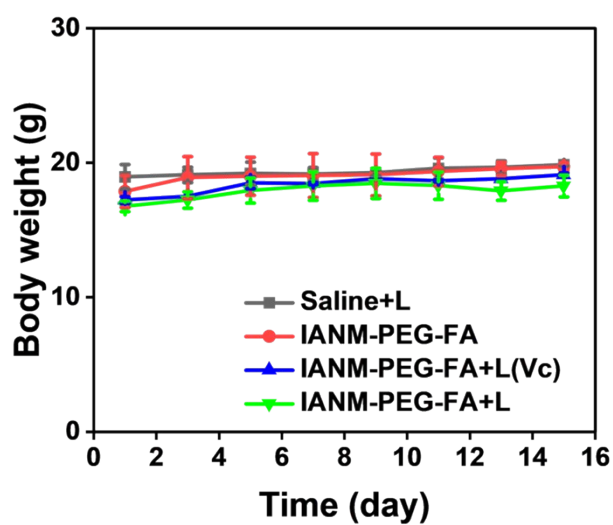

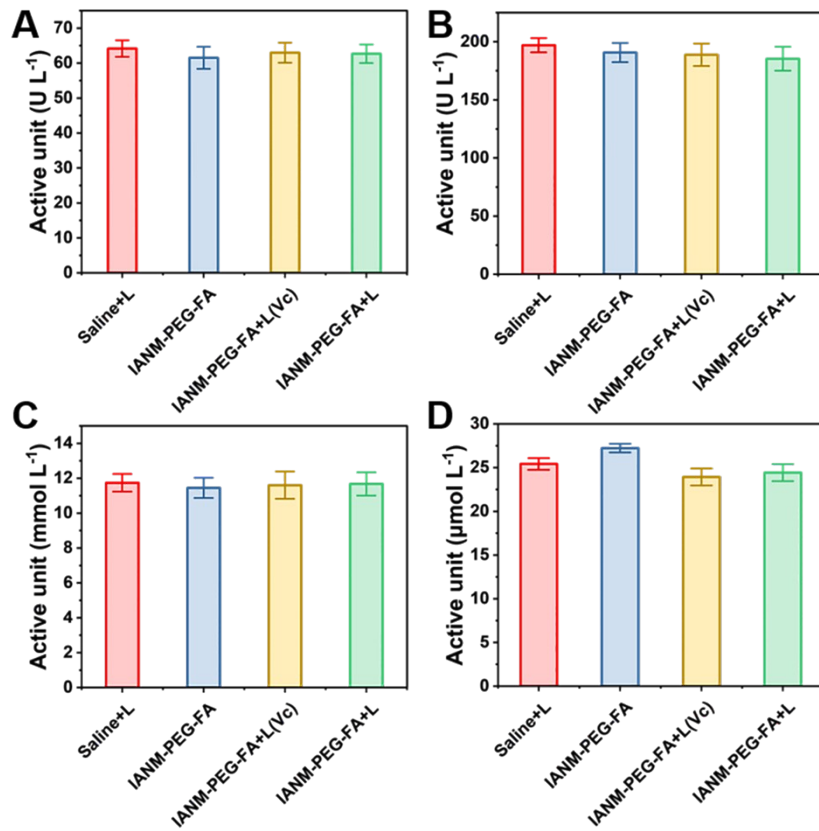**Fig. S12.** Body weight change curves of mice in different treatment groups.

Fig. S13. Liver and kidney function indicator tests. The concentration of ALT (A), AST (B), BUN (C), and CRE (D) in blood after intravenous injection with different specimens.